# Red-emitting Tetra-coordinate Organoboron Chelates: Synthesis, Photophysical Properties, and Fluorescence Microscopy

Vânia F. Pais,[†] Pedro Ramírez-López,[‡] Antonio Romero-Arenas,[‡] Daniel Collado,[§,¶] Francisco Nájera,[§,¶] Ezequiel Pérez-Inestrosa,[§,¶] Rosario Fernández,[#] José M. Lassaletta,[‡] Abel Ros,*[,‡,#] and Uwe Pischel*[,†]

[†] CIQSO – Center for Research in Sustainable Chemistry and Department of Chemistry, University of Huelva, Campus de El Carmen s/n, 21071 Huelva, Spain

[‡] Institute for Chemical Research (CSIC-US) and Innovation-Center in Advanced Chemistry (ORFEO-CINQA), C/Américo Vespucio 49, 41092 Seville, Spain

[§] Department of Organic Chemistry, University of Málaga, IBIMA, Campus Teatinos s/n, 29071 Málaga, Spain

[¶] Andalusian Center for Nanomedicine and Biotechnology – BIONAND, Parque Tecnológico de Andalucía, 29590 Málaga, Spain

[#] Department of Organic Chemistry, University of Seville and Innovation-Center in Advanced Chemistry (ORFEO-CINQA), C/Prof. García González 1, 41012 Seville, Spain

**ABSTRACT:** Seven tetra-coordinate organoboron fluorophores with hetero-biaryl N,O or N,N chelate ligands were prepared and photophysically characterized (in toluene). The electronic variation of the heteroaromatic moiety provided a means for the fine-tuning of the UV/vis-absorption and emission spectra. In the most interesting cases the spectra were re-shifted to maximum absorbance at wavelengths longer than 500 nm and emission maxima between 620 and 660 nm. The pronounced intramolecular charge-transfer character of the dyes yielded large Stokes shifts (3500–5100 $cm^{-1}$), while maintaining appreciable fluorescence quantum yields of up to 0.2 for emission maxima longer than 600 nm. The lipophilic character of the dyes enabled their application as stains of vesicle substructures in confocal fluorescence microscopy imaging.

## INTRODUCTION

The molecular design of fluorescent organoboron architectures has received renewed impulse from their demonstrated utility in optoelectronic applications,[1-3] as sensors and switches,[4-7] or in bioimaging.[8-10] Especially tetra-coordinate boron(III) compounds with bidentate chelating ligands have been in the focus of these efforts.[11-15] The coordinative saturation of the boron center confers increased chemical stability and rigidity, often accompanied by significantly high fluorescence quantum yields. *Par excellence* examples for boron(III) dyes with widespread application in chemical biology and sensing are Bodipy dyes.[4,8,16-21] The fluorescence emission of these compounds can be fine-tuned by manipulation of the substitution pattern, extension of the π-conjugate system, or heteroatom substitution in the chromophore skeleton, among other strategies.[22] Examples for such designs are electron-donor-substituted styryl Bodipy dyes[23] and aza-Bodipy dyes.[24-26] Modifications of the chromophore skeleton also have been proven to lead to pronounced red shifts of the emission in the case of xanthene dyes, leading for example to sila- or carbo-derivatives of fluoresceins or rhodamines.[27-29] The extension of the π-conjugation of the chromophore, such as in naphthofluoresceins[30] or cyanine dyes,[31,32] is an often applied recipe for achieving emission in the red or even near-infrared (NIR) spectral region.[9] Fluorophores with red-shifted absorption and emission spectra are of particular interest in bioimaging, because problems of the penetration depth of excitation light and re-absorption of emitted light by the biological tissue are widely avoided.[33-35]

**Chart 1. Structures and general photophysical properties of azaaromatic-based organoboron chelates**[a]

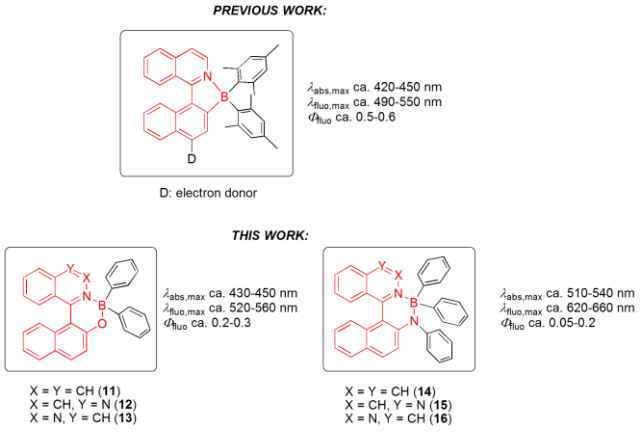


[a] All photophysical data refer to air-equilibrated toluene as solvent.

**Scheme 1. Synthesis of the dyes 11–17.**

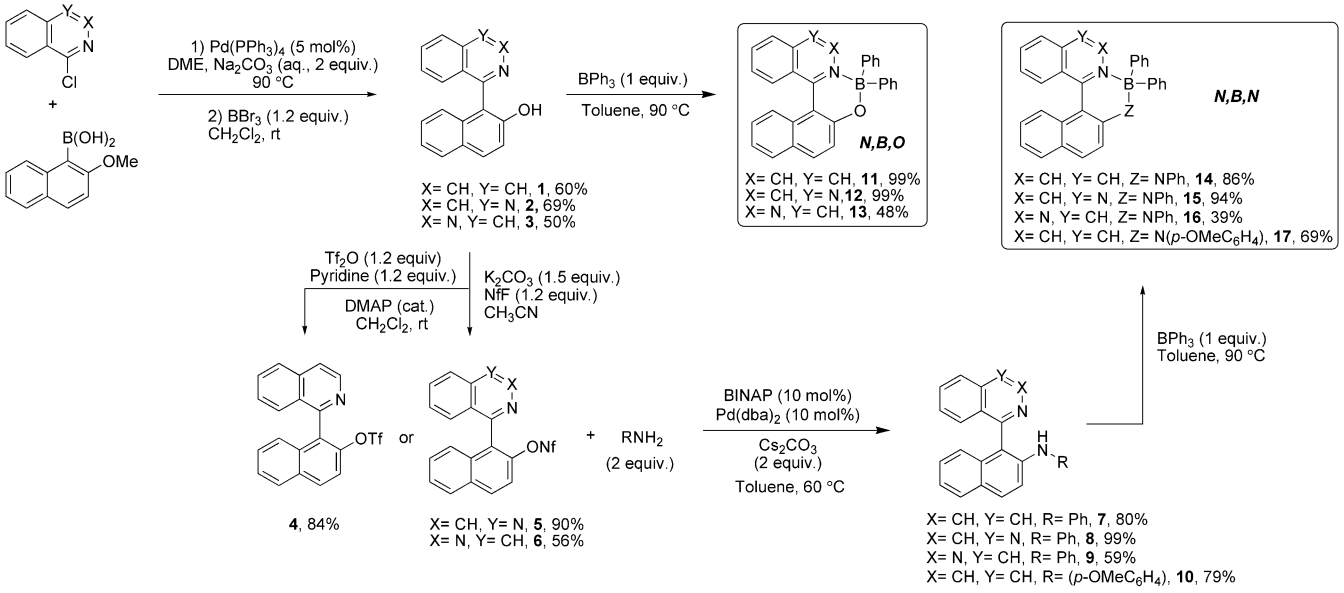


In a recent work we have demonstrated the usefulness of arylisoquinoline-derived N,C ligands for the design of highly fluorescent compounds with applications in bioimaging (see Scheme 1).[10] The photophysical characteristics of these compounds are dominated by intramolecular charge-transfer (ICT) phenomena, providing large Stokes shifts and emissions that can be fine-tuned by electron-donor substitution and/or solvent effects. However, the most red-shifted emission of these fluorophores was still shorter than 600 nm. The desire to force the emission further towards the red spectral region triggered our efforts to synthesize related organoboron fluorophores with an arylisoquinoline skeleton or related *N*-heterocyclic ligands (see Chart 1), such as quinazolines. Interestingly, the latter have been integrated previously in push-pull architectures with interesting emission properties.[36,37]

Additional O- or N-electron-donor substituents were integrated in the expectation of achieving energetically lower lying emissive states. Thereby the above outlined strategies of electronic manipulations of the chromophore skeleton itself and its substitution pattern were synergistically combined. Interestingly, pronounced red shifts of the absorption and fluorescence spectra were obtained for some of the prepared dyes, while maintaining appreciable emission quantum yields of up to 0.2. The implication of ICT processes in the design of red-emitting fluorophores guarantees the desired large Stokes shifts, but unfortunately often leads to very low emission quantum yields. This is a direct consequence of the energy-gap law, favoring non-radiative deactivation of energetically low-lying emissive states, but may find also at least partial explanation in efficient intersystem crossing to close-lying triplet states. Having this in mind, the herein reported quantum yields are very significant.

Finally, the hydrophobic nature and structural shape of these fluorophores led to the prediction of a preferential accumulation in non-polar cell compartments such as vesicle substructures,[38] which indeed was verified by confocal fluorescence microscopy imaging.

## RESULTS AND DISCUSSION

**Synthesis of the Organoboron Dyes 11–17.** The synthesis of the N,B,O-dyes **11**–**13** was carried out starting from the corresponding alcohols **1**–**3**,[39-41] by reaction with $BPh_3$ in anhydrous toluene at 90 °C (Scheme 1). After heating overnight, the purification by conventional flash chromatography or precipitation afforded the dyes **11**–**13** in moderate to excellent yields (48–99%). A similar strategy was employed for the synthesis of the N,B,N-dyes **14**-**17**, where the starting amines **7**–**10** were accessible by a Buchwald-Hartwig coupling reaction[42,43] between the triflate **4**[44] or the nonaflates **5**–**6**[41] and the corresponding aniline. The dyes **14**–**17** were obtained in moderate to excellent yields of 39–94% (see Supporting Information for more details). The identity and purity of the dyes was established by $^{1}H$, $^{13}C$, and $^{11}B$ NMR spectroscopy, as well as electrospray-ionization high-resolution mass spectrometry.

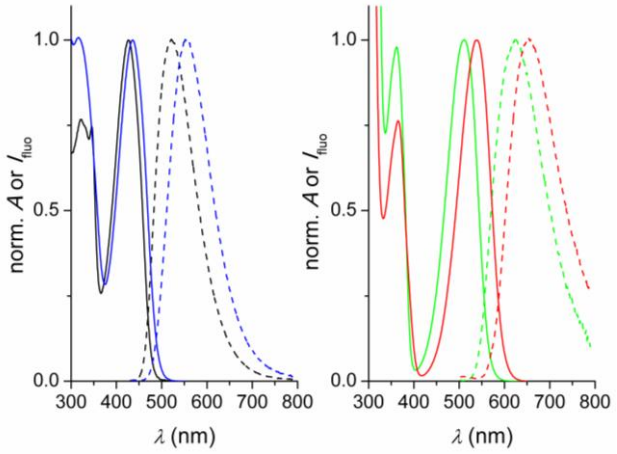


**Figure 1.** Normalized UV/vis absorption spectra (solid lines) and fluorescence spectra (dashed lines) of the compounds **11** (black), **13** (blue), **14** (green), and **15** (red) in air-equilibrated toluene.

**Photophysical Properties.** The UV/vis absorption and fluorescence properties of toluene solutions of the herein prepared dyes are summarized in Table 1 and representative spectra are shown in Figure 1. The absorption spectral properties show a clear dependence on the heterobiaryl skeleton (arylisoquinolines **11**, **14**; arylquinazolines **12**, **15**; arylphthalazines **13**, **16**) for both the N,B,O- and the N,B,N-dye series. In each series the arylquinazoline dyes show the most red-shifted long-wavelength absorption maximum. Furthermore, generally the N,B,N-dyes have more red-shifted absorption (longer than 500 nm) and emission maxima than the N,B,O-dyes, extending to red emission color. The dyes show increased Stokes shifts, varying between *ca*. 3500 and 5100 $cm^{-1}$. The fluorescence quantum yields ($\Phi_{fluo}$) follow clearly the energy-gap law in photochemistry: non-radiative deactivation pathways become more competitive for energetically lower lying emissive states. Hence, the fluorescence quantum yields drop for the N,B,N-dyes, although maintaining still quite appreciable levels considering that these dyes feature emission maxima longer than 600 nm, e.g., $\Phi_{fluo}$ = 0.17 for dye **14**. The introduction of additional electron-donor substitution (i.e., a methoxy group in dye **17**) shifts the absorption and fluorescence maxima somewhat further to the red, but mainly lead to a very accentuated drop of the emission quantum yield, again a direct consequence of the energy-gap law. The fluorescence lifetimes ($\tau_{fluo}$) were measured as being around 9.5 ns for the N,B,O-dyes and are more variable (0.25–6.31 ns) for the N,B,N-dyes.

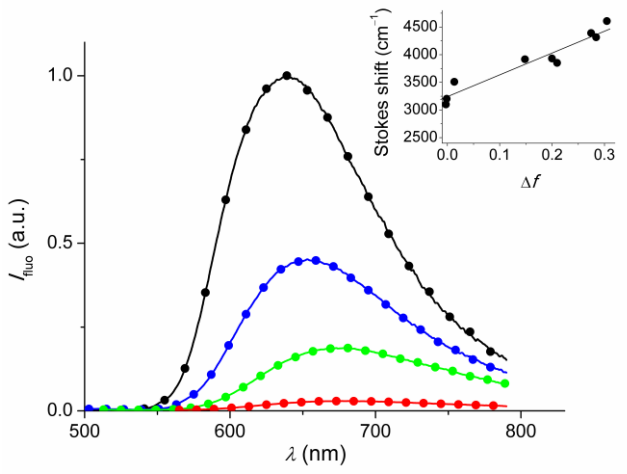


**Figure 2.** Fluorescence spectra of dye **15** in *n*-hexane (black), toluene (blue), chloroform (green), and *N*,*N*-dimethylformamide (red). The spectra are normalized to show the relative emission quantum yields in the different solvents. The inset shows the Lippert-Mataga plot ($n$ = 9, $r^2$ = 0.9151) for dye **15**; see text.

In order to obtain further insights into the nature of the observed fluorescence the solvent effect was studied for selected N,B,N-dyes. Note that the N,B,O-dyes show insufficient chemical stability in solvents such as tetrahydrofuran, *N*,*N*-dimethylformamide and sometimes in acetonitrile. The N,B,N-dyes show a hypsochromic shift (negative solvatochromism) on changing from non-polar toluene to polar acetonitrile, while the emission bands shift bathochromically (positive solvatochromism). As a result the Stokes shift is increased in acetonitrile. This effect is most accentuated for the dyes **15** and **16** for which notable Stokes shifts of 4600 $cm^{-1}$ and 5100 $cm^{-1}$, respectively, were observed. However, expectedly this comes at the expense of a drastically reduced emission quantum yield for these two dyes, being lower than 0.01 in acetonitrile. In order to establish a more detailed trend a series of nine different solvents, addressing aspects such as polarity, hydrogen bonding character, and viscosity, was studied for dye **15** (Figure 2 and detailed data in Supporting Information).

**Table 1. Photophysical properties of N,B,O-dyes 11–13 and N,B,N-dyes 14–17 in air-equilibrated toluene solution.**

| | $\lambda_{abs,max}$ (nm)[a] [$\varepsilon$ ($M^{-1}cm^{-1}$)][b] | $\lambda_{fluo,max}$ (nm)[c] | Stokes shift ($cm^{-1}$) | $\Phi_{fluo}$[d] | $\tau_{fluo}$ (ns)[e] |
|---|---|---|---|---|---|
| **11** | 427 [5000] | 522 | 4481 | 0.32 | 9.47 |
| **12** | 451 [5100] | 543 | 3950 | 0.25 | 9.59 |
| **13** | 436 [3400] | 555 | 5141 | 0.15 | 9.32 |
| **14** | 511 [6300] | 623 | 3777 | 0.17 | 6.31 |
| **15** | 539 [8600] | 654 | 3510 | 0.03 | 1.56 |
| **16** | 524 [2900] | 657 | 4081 | 0.05 | 2.56 |
| **17** | 520 [6700] | 641 | 3978 | <0.01 | 0.25 |

[a] Absorption maximum. [b] Molar absorption coefficient. [c] Fluorescence maximum. [d] Fluorescence quantum yield. [e] Fluorescence lifetime.

Beside the abovementioned positive solvatochromism of the emission spectrum, the following general trends can be derived: (a) protic solvents deactivate the fluorescence practically totally ($\Phi_{fluo} < 10^{-3}$ in methanol), (b) in non-polar solvents the highest fluorescence quantum yields are observed ($\lambda_{max,\ fluo}$ = 641 nm, $\Phi_{fluo}$ = 0.06 in *n*-hexane), (c) increasing viscosity has no influence on the fluorescence ($\lambda_{max,\ fluo}$ = 642 nm, $\Phi_{fluo}$ = 0.07 in decalin). The treatment of the data according to the Lippert-Mataga equation[45-47] yielded a dipole moment change ($\Delta\mu$) between ground and excited state of 10 Debye. This suggests an accentuated intramolecular charge-transfer (ICT) character of the emissive state and is in line with our recent results on N,C chelate tetracoordinate arylisoquinoline organoboron compounds.[10] The ICT character explains the observed large Stokes shifts (see above).

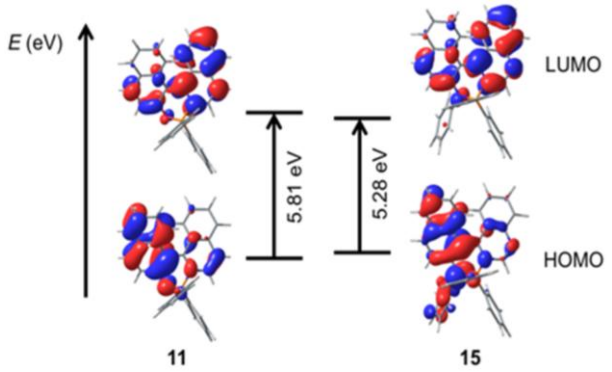


**Figure 3.** HOMO/LUMO isosurface plots and frontier-orbital energies of the dyes **11** and **15**.

The occurrence of ICT was confirmed by time-dependent density-functional theory calculations[48] (CAM-B3LYP/6-311+G(2d,p) level of theory) of **11**, **14**, **15**, and **16** as representative dyes (see Supporting Information). The lowest-energy emission ($S_1 \rightarrow S_0$) corresponds mainly to a LUMO→HOMO transition

(contribution of 95–97%). The contour plots of the frontier orbitals show that the HOMO is mainly located on the naphthyl-derived "half" of the system, while the LUMO has its main contribution from the heteroaromatic moiety; see Figure 3 for the examples of dye **11** and **15**. The natural transition orbital (NTO) analysis yielded the same conclusion of an effective ICT process on excitation of the dyes. This observation resembles similar results that were obtained for related borylated arylisoquinoline (BAI) dyes.[10,49]

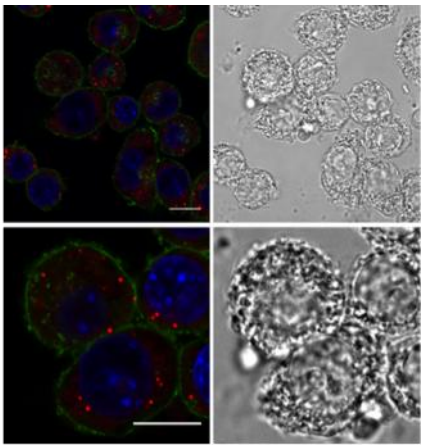

**Figure 4**. Confocal fluorescence microscopy images (left) of N13 mouse microglial cells incubated (for 24 h) with dye **15** (10 μM) – red. The submembrane actin (green) was stained with Atto488-conjugated Phalloidin (0.1 μM) and the nucleus (blue) with Hoechst 33342 (8 μM). The transmission microscopy images are shown on the right side. Scale bars: 10 μm.

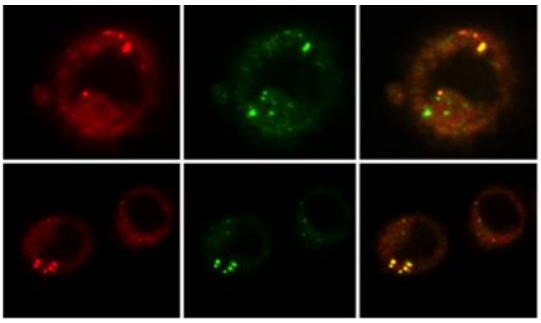

**Figure 5**. Confocal fluorescence microscopy images of N13 mouse microglial cells. On the left the labeling with dye **15** (upper row) and **16** (lower row), both at 30 μM, is shown. The middle images show the corresponding labeling with the lipophilic probe FM4-64 and the overlay is shown on the right.

**Bioimaging Applications.** The negligible fluorescence in protic media as contrasted by the significant fluorescence in non-polar environments prompted us to investigate the use of the lipophilic organoboron N,N-chelates as probes for cellular lipid substructures such as vesicles.[38,50,51] For this purpose the dyes **15** and **16** were incubated with N13 mouse microglial cells. In a first approach viability studies were performed applying a flow cytometry method using simultaneous Hoechst 33342 and propidium iodide staining.[52] This yielded a cell viability rate of 83% following 24 hours of incubation for both dyes at a concentration of 10 μM. These data were confirmed by high-throughput screening with automated microscopy using the same nuclear stains: 86% viability for **15** and 88% for **16** after 24 hours incubation.

In Figure 4 images of N13 cells stained with dye **15**, Hoechst 33342 as marker of the cell nucleus, and Atto488-conjugated Phalloidin as marker for submembrane actin are shown. For many organic fluorophores a homogeneous cytoplasmic accumulation is typical, while for our dyes just a very weak "cloud-like" fluorescence was evident. This is in accordance with the strongly deactivated fluorescence of the dye in polar (protic) media. However, a clear light-up behavior for the dye accumulation in some small intracellular substructures was observed. Having in mind the considerably higher fluorescence in non-polar environments, this is interpreted as the accumulation in vesicle-like substructures. Co-localization imaging (Figure 5) demonstrated the specific accumulation of the investigated dyes **15** and **16** in structures that are also marked by the liphophilic styryl dye FM4-64.[53]

## CONCLUSIONS

In summary, lipophilic tetra-coordinate N,O- and N,N-chelate organoboron dyes show distinct photophysical properties that enable their application as vesicle stains in confocal fluorescence microscopy imaging. On the one hand, the N,O-chelates show green-to-yellow emission with quantum yields of up to 0.3 in toluene. On the other hand, the N,N-chelates are characterized by fluorescence emission maxima longer than 600 nm, maintaining significant fluorescence quantum yields (up to 0.2 in toluene). The emission quantum yields in the N,B,N series are generally lower than in the N,B,O series, being a direct consequence of the energy gap law and more dominant non-radiative deactivation pathways. The large Stokes shifts of *ca*. 3500–5100 $cm^{-1}$ (in toluene) typical for the herein verified intramolecular charge-transfer phenomena, and the pronounced solvent-dependence of the emission (especially of the N,B,N dyes) are additional attributes of the functional characteristics.

## EXPERIMENTAL SECTION

**General Methods.** $^{1}H$ NMR spectra were recorded at 400 or 500 MHz; $^{13}C$ NMR spectra were recorded at 100 or 125 MHz with the solvent peak used as the internal reference (7.26 and 77.0 ppm for $^{1}H$ and $^{13}C$, respectively). $^{11}B$ NMR spectra were recorded with complete proton decoupling at 128 MHz using $BF_3{\cdot}Et_2O$ (0.00 ppm for $^{11}B$-NMR) as an external standard. Electrospray-ionization (EI) high-resolution mass spectra were obtained with a QTRAP mass spectrometer (hybrid triple quadrupole/linear ion trap mass spectrometer). Column chromatography was performed on silica gel. Analytical TLC was performed on aluminium backed plates (1.5 × 5 cm) precoated (0.25 mm) with silica gel. Compounds were visualized by exposure to UV light or by dipping the plates in a solution of 5% $(NH_4)_2Mo_7O_{24}{\cdot}4H_2O$ in 95% EtOH (w/v) or followed by heating.

Anhydrous 1,4-dioxane and THF were obtained by distillation from sodium using benzophenone as indicator. $Pd(dba)_2$, $BPh_3$, BINAP ligand, aniline, and *p*-anisidine were commercially available. The alcohols **1-3**,[39-41] the triflate **4**,[44] and the nonaflates **5-6**[41] are known compounds. The NMR spectra of the herein analogously prepared compounds were found to resemble the published data.

The solvents for the photophysical measurements were of spectroscopic quality and used as received.

**General Procedure for the Synthesis of 7–10**. A flamed-dried Schlenk tube was charged with the corresponding nonaflate **4-6** (0.2 mmol), $Cs_2CO_3$ (0.4 mmol, 130.2 mg), $Pd(dba)_2$ (10 mol%, 11.6 mg) and BINAP (10 mol%, 12.4 mg). After three cycles of vacuum-argon flushing, deoxygenated dry toluene (4 mL) and the appropriate amine (0.4 mmol) were sequentially added in this order. The reaction mixture was stirred at 60°C for 24 hours, then cooled down to room temperature, and filtered through a celite pad. The solvent was removed under vacuum and the resulting residue was purified by column chromatography on silica gel.

**Compound 7**. Following the general procedure starting from **4**; purification by flash chromatography ($CH_2Cl_2$/EtOAc 50:1→10:1) gave **7** (55 mg, 80%) as a yellow foam. $^1$H NMR (400 MHz, $CDCl_3$): δ 8.78 (d, 1H, *J* = 5.8 Hz), 7.93 (d, 1H, *J* = 8.3 Hz), 7.88 (d, 1H, *J* = 9.0 Hz), 7.83 (d, 1H, *J* = 8.0 Hz), 7.78 (dd, 1H, *J* = 5.7 and 0.6 Hz), 7.68 (ddd, 1H, *J* = 8.2, 6.9, and 1.2 Hz), 7.71 (d, 1H, *J* = 9.0 Hz), 7.60 (dd, 1H, *J* = 8.5 and 0.8 Hz), 7.39 (ddd, 1H, *J* = 8.4, 7.0, and 1.2 Hz), 7.30 (ddd, 1H, *J* = 8.1, 6.9, and 1.2 Hz), 7.23–7.16 (m, 3H), 7.02–6.97 (m, 2H), 6.95–6.91 (m, 1H), 6.88 (t, 1H, *J* = 7.3 Hz), 6.05 (s, 1H) ppm. $^{13}$C NMR (100 MHz, $CDCl_3$): δ 158.6, 143.1, 142.9, 139.4, 136.9, 134.0, 130.7, 129.7, 129.4, 129.3, 128.6, 128.2, 127.8, 127.5, 127.2, 126.7, 124.9, 123.5, 121.9, 121.4, 120.7, 119.1, 118.8 ppm. HRMS (ESI) calcd. $C_{25}H_{19}N_2$ for ($M+H^+$) 347.1543. Found 347.1537. Anal. calcd for $C_{25}H_{18}N_2$: C, 86.68; H, 5.24; N, 8.09. Found: C, 86.65; H, 5.26; N, 8.21.

**Compound 8**. Following the general procedure starting from **5**; purification by flash chromatography (*n*-hexane/EtOAc 3:1) gave **8** (69 mg, 99%) as a yellow foam. $^1$H NMR (400 MHz, $CDCl_3$): δ 9.45 (s, 1H), 8.08 (d, 1H, *J* = 8.5 Hz), 7.91 (d, 1H, *J* = 9.0 Hz), 7.86 (ddd, 1H, *J* = 8.5, 6.9, and 1.4 Hz), 7.84 (d, 1H, *J* = 8.0 Hz), 7.71 (d, 1H, *J* = 9.1 Hz), 7.66–7.59 (m, 1H), 7.44 (ddd, 1H, *J* = 8.3, 7.0, and 1.1 Hz), 7.33 (ddd, 1H, *J* = 8.0, 6.9, and 1.1 Hz), 7.27–7.17 (m, 3H), 7.07–7.01 (m, 2H), 6.97 (d, 1H, *J* = 8.5 Hz), 6.92 (t, 1H, *J* = 1.0 Hz), 6.47 (br s, 1H) ppm. $^{13}$C NMR (100 MHz, $CDCl_3$): δ 167.7, 155.1, 150.9, 142.3, 139.5, 134.4, 133.1, 130.6, 129.3, 129.1, 128.9, 128.2, 128.1, 127.1, 127.0, 125.0, 124.3, 123.8, 121.7, 119.2, 119.1, 118.9 ppm. HRMS (ESI) calcd. for $C_{24}H_{18}N_3$ ($M+H^+$) 348.1495. Found 348.1500. Anal. calcd for $C_{24}H_{17}N_3$: C, 82.97; H, 4.93; N, 12.10. Found: C, 82.89; H, 5.21; N, 11.89.

**Compound 9**. Following the general procedure starting from **6**; purification by flash chromatography (*n*-hexane/EtOAc 3:1) gave **9** (41 mg, 59%) as a yellow amorphous solid. Mp: 224–226 ºC. $^1$H NMR (400 MHz, $CDCl_3$): δ 9.63 (s, 1H), 8.05 (d, 1H, *J* = 8.1 Hz), 7.95–7.86 (m, 2H), 7.85 (d, 1H, *J* = 8.1 Hz), 7.73 (d, 1H, *J* = 9.1 Hz), 7.69 (t, 1H, *J* = 7.3 Hz), 7.55 (d, 1H, *J* = 8.3 Hz), 7.32 (t, 1H, *J* = 7.3 Hz), 7.25–7.13 (m, 3H), 6.99 (d, 2H, *J* = 7.8 Hz), 6.93 (d, 1H, *J* = 8.5 Hz), 6.88 (t, 1H, *J* = 7.3 Hz), 6.37 (br s, 1H) ppm. $^{13}$C NMR (100 MHz, $CDCl_3$): δ 158.7, 151.1, 142.5, 139.8, 133.7, 132.8, 130.3, 129.2, 128.1, 127.0, 126.9, 126.8, 126.6, 126.2, 124.5, 123.7, 121.4, 119.3, 118.6, 118.5 ppm. HRMS (ESI) calcd. for $C_{24}H_{18}N_3$ ($M+H^+$) 348.1495. Found 348.1491. Anal. calcd for $C_{24}H_{17}N_3$: C, 82.97; H, 4.93; N, 12.10. Found: C, 82.61; H, 5.33; N, 11.71.

**Compound 10**. Following the general procedure starting from **4**; purification by flash chromatography (toluene/EtOAc 10:1) gave **10** (59 mg, 79%) as a light yellow foam. $^1$H NMR (400 MHz, $CDCl_3$): δ 8.78 (d, 1H, *J* = 5.7 Hz), 7.94 (d, 1H, *J* = 8.3 Hz), 7.83 (d, 1H, *J* = 9.1 Hz), 7.80 (m, 2H), 7.70 (ddd, 1H, *J* = 8.0, 6.9, and 1.1 Hz), 7.64 (d, 1H, *J* = 8.3 Hz), 7.49 (d, 1H, J = 9.1 Hz), 7.42 (ddd, 1H, *J* = 8.2, 7.0, and 1.0 Hz), 7.28–7.22 (m, 1H), 7.18 (ddd, 1H, *J* = 8.2, 6.9, and 1.3 Hz), 7.03–6.95 (m, 2H), 6.88 (d, 1H, *J* = 8.4 Hz), 6.82–6.75 (m, 2H), 5.76 (br s, 1H), 3.75 (s, 3H) ppm. $^{13}$C NMR (100 MHz, $CDCl_3$): δ 158.6, 155.6, 142.8, 141.4, 137.1, 135.7, 134.0, 131.0, 129.9, 128.7, 128.2, 127.9, 127.7, 127.2, 126.8, 124.5, 123.0, 120.8, 119.1, 117.8, 114.7, 55.7 ppm. HRMS (ESI) calcd. for $C_{26}H_{21}N_2O$ ($M+H^+$) 377.1648. Found 377.1641. Anal. calcd for $C_{26}H_{20}N_2O$: C, 82.95; H, 5.36; N, 7.44. Found: C, 82.98; H, 5.72; N, 7.29.

**General procedure for the synthesis of 11–17**. A dried Schlenk tube was charged with the substrate **1**–**3** or **7**–**10** (0.1–0.2 mmol) and $BPh_3$ (1 equiv.). After three cycles of vacuum-argon flushing 1 mL of dried-deoxygenated toluene was added. The reaction mixture was stirred at 90 °C until reaching maximum consumption of the starting material (TLC monitoring), then cooled down to room temperature, and finally concentrated to dryness. The crude products were purified by column chromatography on silica gel (*n*-hexane/EtOAc, toluene/EtOAc or $CH_2Cl_2$/EtOAc mixtures as eluents) or by washing with *n*-hexane/EtOAc mixtures.

**Compound 11**. Following the general procedure starting from **1** (0.1 mmol, 27 mg) and heating for 18 hours; flash chromatography on silica gel (*n*-hexane/EtOAc 1:3) gave **11** (43 mg, 99%) as a yellow foam. $^1$H NMR (400 MHz, $CDCl_3$): δ 8.05 (d, 1H, *J* = 5.6 Hz), 7.94–7.88 (m, 3H), 7.83 (t, 1H, *J* = 7.8 Hz), 7.73 (d, 1H, *J* = 8.8 Hz), 7.65 (d, 1H, *J* = 6.6 Hz), 7.48 (d, 1H, *J* = 8.8 Hz), 7.45 (t, 1H, *J* = 8.2 Hz), 7.39–7.37 (m, 2H), 7.32–7.25 (m, 7H), 7.14 (ddd, 1H, *J* = 8.6, 6.6, and 1.2 Hz), 7.04 (t, 2H, *J* = 7.0 Hz), 6.97 (t, 1H, *J* = 7.0 Hz) ppm. $^{13}$C NMR (100 MHz, $CDCl_3$): δ 163.4, 151.5, 137.6, 136.1, 134.9, 134.4, 132.9, 132.3, 131.9, 131.0, 128.5, 128.4, 127.7, 127.6, 127.0, 126.9, 126.7, 126.1, 125.5, 125.1, 124.7, 123.3, 121.7, 119.6, 113.8 ppm, (C–B not observed). $^{11}$B NMR (128 MHz, $CDCl_3$): δ 6.1 (br s) ppm. HRMS (ESI) calcd. for $C_{31}H_{23}BNO$ ($M+H^+$) 436.1867. Found 436.1847.

**Compound 12**. Following the general procedure starting from **2** (0.2 mmol, 54 mg) and heating for 20 hours; the reaction crude was triturated with a *n*-hexane/EtOAc 3:1 mixture to give **12** (88 mg, 99%) as a yellow-orange foam. $^1$H NMR (400 MHz, $CDCl_3$): δ 8.82 (s, 1H), 8.11 (d, 1H, *J* = 8.2 Hz), 7.99 (ddd, 1H, *J* = 8.2, 6.9, and 1.2 Hz), 7.97 (d, 1H, *J* = 9.0 Hz), 7.93 (d, 1H, *J* = 8.6 Hz), 7.74 (d, 1H, *J* = 7.6 Hz), 7.49 (ddd, 1H, *J* = 8.2, 7.0, and 1.1 Hz), 7.46 (d, 1H, *J* = 8.9 Hz), 7.42–7.38 (m, 3H), 7.34-7.29 (m, 4H), 7.24–7.21 (m, 3H), 7.08 (t, 2H, *J* = 7.0 Hz), 7.02 (t, 1H, *J* = 7.2 Hz) ppm. $^{13}$C NMR (100 MHz, $CDCl_3$): δ 165.8, 155.9, 150.6, 147.9, 137.7, 136.2, 134.3, 132.1, 131.8, 130.1, 128.9, 128.7, 128.6, 128.1, 127.8, 127.4, 126.9, 125.9, 124.7, 124.3, 121.8, 119.8, 112.5 ppm, (C–B not observed). $^{11}$B NMR (128 MHz, $CDCl_3$): δ 5.5 (br s) ppm. HRMS (ESI) calcd. for $C_{30}H_{22}BN_2O$ ($M+H^+$) 437.1820. Found 437.1799.

**Compound 13**. Following the general procedure starting from **3** (0.2 mmol, 54 mg) and heating for 48 hours, still starting material was remaining. Flash chromatography on silica gel (*n*-hexane/EtOAc 2:1→1:1) gave **13** (40 mg, 48%) as a yellow foam. $^1$H NMR (400 MHz, $CDCl_3$): δ 9.30 (s, 1H), 8.07–8.03 (m, 2H), 7.99 (d, 1H, *J* = 9.0 Hz), 7.96 (d, 1H, *J* = 8.9 Hz), 7.78–7.74 (m, 2H), 7.54 (d, 1H, *J* = 8.9 Hz), 7.44 (d, 2H, *J* = 6.7 Hz), 7.36 (d, 2H, *J* = 6.2 Hz), 7.30–7.21 (m, 5H), 7.16 (ddd, 1H, *J* = 8.2, 6.8, and 1.2 Hz), 7.08 (t, 2H, *J* = 7.4 Hz), 7.01 (t, 1H, *J* = 7.2 Hz) ppm. $^{13}$C NMR (100 MHz, $CDCl_3$): δ 164.2, 151.1, 148.4, 136.3, 134.7, 133.9, 132.5, 132.4, 131.6, 130.0, 128.8, 128.6, 127.5, 127.0, 126.8, 126.7, 126.5, 125.7, 125.6, 124.2, 123.7, 122.0, 110.8 ppm, (C–B not observed). $^{11}$B NMR (128 MHz, $CDCl_3$): δ 6.1 (br s) ppm. HRMS (ESI) calcd. for $C_{30}H_{22}BN_2O$ ($M+H^+$) 437.1820. Found 437.1801.

**Compound 14**. Following the general procedure starting from **7** (0.1 mmol, 34.6 mg) and heating for 7 hours; flash chromatography on silica gel (*n*-hexane/EtOAc 3:1) gave **14** (44 mg, 86%) as a deep red foam. $^{1}$H NMR (400 MHz, $CDCl_3$): δ 8.00 (d, 1H, *J* = 6.7 Hz), 7.92 (d, 1H, *J* = 8.6 Hz), 7.87 (d, 1H, *J* = 8.0 Hz), 7.75 (t, 1H, *J* = 7.8 Hz), 7.63 (d, 1H, *J* = 9.2 Hz), 7.61 (d, 1H, *J* = 8.0 Hz), 7.52 (d, 1H, *J* = 6.7 Hz), 7.38 (ddd, 1H, *J* = 8.3 6.9 and 1.0 Hz), 7.32 (d, 1H, *J* = 9.2 Hz), 7.28–7.26 (m, 2H), 7.20–7.15 (m, 4H), 7.13 (ddd, 1H, *J* = 7.9, 6.9 and 1.2 Hz), 7.08–6.91 (m, 9H), 6.81–6.80 (m, 2H) ppm. $^{13}$C NMR (100 MHz, $CDCl_3$): δ 153.4, 151.2, 147.5, 136.9, 136.3, 133.3, 133.1, 132.7, 132.1, 131.4, 129.2, 128.0, 127.9, 127.3, 126.8, 126.6, 126.0, 125.5, 125.1, 125.0, 123.0, 122.6, 121.1, 117.9, 113.2 ppm, (C–B not observed). $^{11}$B NMR (128 MHz, $CDCl_3$): δ 3.8 (br s) ppm. HRMS (ESI) calcd. for $C_{37}H_{28}BN_2$ ($M+H^+$) 511.2340. Found 511.2325. Anal. calcd for $C_{37}H_{27}BN_2$: C, 87.06; H, 5.33; N, 5.49. Found: C, 87.09; H, 5.82; N, 5.23.

**Compound 15**. Following the general procedure starting from **8** (0.1 mmol, 34.7 mg) and heating for 12 hours; flash chromatography on silica gel (toluene) gave **15** (48 mg, 94%) as a purple foam. $^{1}$H NMR (400 MHz, $CDCl_3$): δ 8.75 (s, 1H), 8.00 (d, 1H, *J* = 8.0 Hz), 7.89 (d, 1H, *J* = 8.5 Hz), 7.85 (ddd, 1H, *J* = 8.3, 7.0, and 1.2 Hz), 7.65 (d, 1H, *J* = 9.3 Hz), 7.61 (d, 1H, *J* = 7.9 Hz), 7.37 (ddd, 1H, *J* = 8.3, 7.1, and 1.1 Hz), 7.29–7.17 (m, 8H), 7.09–6.93 (m, 9H), 6.90–6.88 (m, 2H) ppm. $^{13}$C NMR (100 MHz, $CDCl_3$): δ 155.1, 153.5, 149.2, 147.9, 146.3, 135.4, 134.7, 133.1, 133.0, 130.2, 129.2, 128.5, 128.2, 128.1, 127.5, 127.4, 127.0, 126.8, 126.7, 126.4, 125.4, 125.3, 124.3, 123.8, 120.6, 120.2, 111.3 ppm, (C–B not observed). $^{11}$B NMR (128 MHz, $CDCl_3$): δ 2.9 (br s) ppm. HRMS (ESI) calcd. for $C_{36}H_{27}BN_3$ ($M+H^+$) 512.2293. Found 512.2276. Anal. calcd for $C_{36}H_{26}BN_3$: C, 84.55; H, 5.12; N, 8.22. Found: C, 84.42; H, 5.20; N, 8.25.

**Compound 16**. Following the general procedure starting from **13** (0.1 mmol, 34.7 mg), and heating for 72 hours, still starting material was remaining. Flash chromatography on silica gel (*n*-hexane/EtOAc 3:1) gave **16** (20 mg, 39%) as a purple foam. $^{1}$H NMR (400 MHz, $CDCl_3$): δ 9.16 (d, 1H, *J* = 0.8 Hz), 7.99 (d, 1H, *J* = 8.2 Hz), 7.98 (dd, 1H, *J* = 7.5 and 1.4 Hz), 7.92 (ddd, 1H, *J* = 8.0, 7.0, and 1.0 Hz), 7.69–7.63 (m, 3H), 7.46–7.44 (m, 2H), 7.29 (d, 1H, *J* = 9.2 Hz), 7.17 (ddd, 1H, *J* = 8.0, 6.8, and 1.2 Hz), 7.10–7.05 (m, 4H), 7.03–6.91 (m, 11H) ppm. $^{13}$C NMR (100 MHz, $CDCl_3$): δ 153.9, 148.8, 147.1, 147.0, 135.9, 133.9, 133.6, 133.4, 132.8, 132.0, 130.2, 128.2, 128.0, 127.5, 127.2, 126.6, 126.4, 126.3, 126.2, 125.3, 125.2, 124.6, 123.6, 123.1, 121.1, 109.3 ppm, (C–B not observed). $^{11}$B NMR (128 MHz, $CDCl_3$): δ 4.0 (br s) ppm. HRMS (ESI) calcd. for $C_{36}H_{26}BN_3Na$ ($M+Na^+$) 534.2112. Found 534.2102.

**Compound 17**. Following the general procedure starting from **10** (0.1 mmol, 37.6 mg) and heating for 12 hours; flash chromatography on silica gel (*n*-hexane/$CH_2Cl_2$ 1:3) gave **17** (37 mg, 69%) as a purple foam. $^{1}$H NMR (400 MHz, $CDCl_3$): δ 7.98 (d, 1H, *J* = 6.7 Hz), 7.91 (d, 1H, *J* = 8.7 Hz), 7.86 (d, 1H, *J* = 8.1 Hz), 7.73 (t, 1H, *J* = 7.9 Hz), 7.62 (d, 1H, *J* = 9.2 Hz), 7.60 (d, 1H, *J* = 7.8 Hz), 7.50 (d, 1H, *J* = 6.7 Hz), 7.36 (t, 1H, *J* = 8.1 Hz), 7.28–7.24 (m, 3H), 7.13–6.93 (m, 12H), 7.50 (d, 2H, *J* = 8.8 Hz), 6.48 (dd, 1H, *J* = 8.8 and 2.8 Hz), 3.72 (s, 3H) ppm. $^{13}$C NMR (100 MHz, $CDCl_3$): δ 155.6, 153.7, 151.0, 140.8, 136.9, 136.2, 133.4, 133.2, 132.7, 132.0, 131.4, 129.9, 128.2, 127.9, 127.2, 127.1, 126.8, 126.6, 126.0, 125.9, 125.4, 125.1, 125.0, 122.5, 121.0, 117.7, 113.7, 112.9, 112.6, 55.3 ppm, (C–B not observed). $^{11}$B NMR (128 MHz, $CDCl_3$): δ 3.7 (br s) ppm. HRMS (ESI) calcd. for $C_{38}H_{30}BN_2O$ ($M+H^+$) 541.2446. Found 541.2435. Anal. calcd for $C_{38}H_{29}BN_2O$: C, 84.45; H, 5.41; N, 5.18. Found: C, 84.56; H, 5.33; N, 5.02.

**Photophysical Measurements**. The photophysical data were obtained for air-equilibrated solutions at room temperature. The UV/Vis-absorption spectra and the fluorescence spectra were recorded with standard instrumentation. The emission spectra were corrected for the sensitivity of the photomultiplier detector. The fluorescence quantum yields were determined with 4-amino-*N*-propyl-1,8-naphthalimide ($\Phi_{fluo}$ = 0.48 in acetonitrile)[38] or tris(2,2′-bipyridyl)dichlororuthenium(II) hexahydrate ($\Phi_{fluo}$ = 0.028 in air-equilibrated water)[54] as reference and corrected for refractive index differences of the used solvents. The lifetime measurements were performed by means of time-correlated single-photon-counting with picosecond pulsed diode laser ($\lambda$ = 442 nm, pulse width fwhm 78 ps, $\lambda$ = 482 nm, pulse width fwhm 101 ps) as excitation sources.

**Confocal Fluorescence Microscopy**. N13 mouse microglia cells were grown to 60% confluence on 8 well slides in complete medium (CM) containing Roswell Park Memorial Institute 1640 medium supplemented with 10% fetal calf serum, penicillin (100 units $mL^{-1}$), streptomycin (100 µg $mL^{-1}$), and gentamicin (1.25 units $mL^{-1}$). Test compounds were diluted in fresh CM, added to each well and cultured under optimal conditions (37 ºC and 5% $CO_2$ in a humidified incubator) for a further 24 hours. Live cells were examined using a microscope stage-top incubator to maintain cells under optimal conditions (37 ºC, 5% $CO_2$ and humidity) during imaging. Co-staining, using the lipophilic marker FM4-64FX, was achieved by adding it directly to the culture medium at a 5 µg/mL final concentration. For fixation, cells were washed with pre-warmed PBS, incubated with 4% paraformaldehyde in phosphate buffer saline (PBS) for 20 minutes at room temperature and washed three times with PBS. Sub-membrane actin and nuclei (DNA) were labelled for 20 minutes with 0.1 µM Atto488-conjugated Phalloidin and 8 µM Hoechst 33342, respectively. Live and fixed cells were analyzed using an inverted microscope, a 25× NA 0.95 Plan-APO water immersion objective, and a laser scanning confocal system. In live cells, the emission of the organoboron dyes and FM4-64FX were detected using 561 and 594 nm excitation wavelengths with 569–635 and 712–774 nm detection windows, respectively. In fixed cells Hoechst 33258, ATTO488-Phalloidin and the organoboron dyes were detected using 405, 488 and 561 nm excitation wavelengths with 415–470, 493–555 and 668–690 nm detection windows, respectively. Channels were acquired sequentially and configured to avoid crosstalk between different fluorophores.

## ASSOCIATED CONTENT

**Supporting Information**. Copies of $^{1}$H and $^{13}$C NMR spectra, details on DFT calculations, additional photophysical data. This material is available free of charge via the Internet at http://pubs.acs.org.

## AUTHOR INFORMATION

### Corresponding Author

* E-mail (U.P.): uwe.pischel@diq.uhu.es
* E-mail (A.R.): abel.ros@iiq.csic.es

### Notes

The authors declare no competing financial interest.

## ACKNOWLEDGEMENTS

The funding by the Spanish Ministry of Economy and Competitiveness (grants CTQ2014-54729-C2-1-P for U.P., CTQ2013-

48164-C2-1-P, CTQ2013-48164-C2-2-P for A.R., CTQ2013-41339-P and CTQ2015-71896-REDT for E.P.I., Ramón y Cajal contract RYC-2013-12585 for A.R.), the European Union (FEDER), and the Andalusian Government (grants 2012/FQM-2140 for U.P., 2009/FQM-4537 and 2012/FQM-1078 for A.R., postdoctoral contract for V.F.P.) is acknowledged. Furthermore, we are thankful for the provided access to the Supercomputing and Bioinformatics Center (University of Málaga).

## REFERENCES

(1) Wakamiya, A.; Taniguchi, T.; Yamaguchi, S. *Angew. Chem. Int. Ed.* **2006**, *45*, 3170-3173.

(2) Entwistle, C. D.; Marder, T. B. *Angew. Chem. Int. Ed.* **2002**, *41*, 2927-2931.

(3) Rao, Y.-L.; Wang, S. *Inorg. Chem.* **2011**, *50*, 12263-12274.

(4) Bozdemir, O. A.; Guliyev, R.; Buyukcakir, O.; Selcuk, S.; Kolemen, S.; Gulseren, G.; Nalbantoglu, T.; Boyaci, H.; Akkaya, E. U. *J. Am. Chem. Soc.* **2010**, *132*, 8029-8036.

(5) Kowada, T.; Maeda, H.; Kikuchi, K. *Chem. Soc. Rev.* **2015**, *44*, 4953-4972.

(6) Rao, Y.-L.; Amarne, H.; Zhao, S.-B.; McCormick, T. M.; Martić, S.; Sun, Y.; Wang, R.-Y.; Wang, S. *J. Am. Chem. Soc.* **2008**, *130*, 12898-12900.

(7) Baik, C.; Hudson, Z. M.; Amarne, H.; Wang, S. *J. Am. Chem. Soc.* **2009**, *131*, 14549-14559.

(8) Kolemen, S.; Işık, M.; Kim, G. M.; Kim, D.; Geng, H.; Buyuktemiz, M.; Karatas, T.; Zhang, X.-F.; Dede, Y.; Yoon, J.; Akkaya, E. U. *Angew. Chem. Int. Ed.* **2015**, *54*, 5340-5344.

(9) Lavis, L. D.; Raines, R. T. *ACS Chem. Biol.* **2014**, *9*, 855-866.

(10) Pais, V. F.; Alcaide, M. M.; Rodríguez-López, R.; Collado, D.; Nájera, F.; Pérez-Inestrosa, E.; Álvarez, E.; Lassaletta, J. M.; Fernández, R.; Ros, A.; Pischel, U. *Chem. Eur. J.* **2015**, *21*, 15369-15376.

(11) Frath, D.; Massue, J.; Ulrich, G.; Ziessel, R. *Angew. Chem. Int. Ed.* **2014**, *53*, 2290-2310.

(12) Frath, D.; Azizi, S.; Ulrich, G.; Retailleau, P.; Ziessel, R. *Org. Lett.* **2011**, *13*, 3414-3417.

(13) Niu, S.-l.; Massif, C.; Ulrich, G.; Renard, P.-Y.; Romieu, A.; Ziessel, R. *Chem. Eur. J.* **2012**, *18*, 7229-7242.

(14) Frath, D.; Poirel, A.; Ulrich, G.; De Nicola, A.; Ziessel, R. *Chem. Commun.* **2013**, *49*, 4908-4910.

(15) Roubinet, B.; Massif, C.; Moreau, M.; Boschetti, F.; Ulrich, G.; Ziessel, R.; Renard, P.-Y.; Romieu, A. *Chem. Eur. J.* **2015**, *21*, 14589-14601.

(16) Coskun, A.; Akkaya, E. U. *J. Am. Chem. Soc.* **2006**, *128*, 14474-14475.

(17) Loudet, A.; Burgess, K. *Chem. Rev.* **2007**, *107*, 4891-4932.

(18) Zheng, Q.; Xu, G.; Prasad, P. N. *Chem. Eur. J.* **2008**, *14*, 5812-5819.

(19) Ulrich, G.; Ziessel, R.; Harriman, A. *Angew. Chem. Int. Ed.* **2008**, *47*, 1184-1201.

(20) Juárez, L. A.; Barba-Bon, A.; Costero, A. M.; Martínez-Máñez, R.; Sancenón, F.; Parra, M.; Gaviña, P.; Terencio, M. C.; Alcaraz, M. J. *Chem. Eur. J.* **2015**, *21*, 15486-15490.

(21) Juárez, L. A.; Costero, A. M.; Parra, M.; Gil, S.; Sancenón, F.; Martínez-Máñez, R. *Chem. Commun.* **2015**, *51*, 1725-1727.

(22) Lu, H.; Mack, J.; Yang, Y.; Shen, Z. *Chem. Soc. Rev.* **2014**, *43*, 4778-4823.

(23) Rurack, K.; Kollmannsberger, M.; Daub, J. *Angew. Chem. Int. Ed.* **2001**, *40*, 385-387.

(24) Killoran, J.; Allen, L.; Gallagher, J. F.; Gallagher, W. M.; O'Shea, D. F. *Chem. Commun.* **2002**, 1862-1863.

(25) Loudet, A.; Bandichhor, R.; Burgess, K.; Palma, A.; McDonnell, S. O.; Hall, M. J.; O'Shea, D. F. *Org. Lett.* **2008**, *10*, 4771-4774.

(26) Le Guennic, B.; Maury, O.; Jacquemin, D. *Phys. Chem. Chem. Phys.* **2012**, *14*, 157-164.

(27) Koide, Y.; Urano, Y.; Hanaoka, K.; Piao, W.; Kusakabe, M.; Saito, N.; Terai, T.; Okabe, T.; Nagano, T. *J. Am. Chem. Soc.* **2012**, *134*, 5029-5031.

(28) Grimm, J. B.; Sung, A. J.; Legant, W. R.; Hulamm, P.; Matlosz, S. M.; Betzig, E.; Lavis, L. D. *ACS Chem. Biol.* **2013**, *8*, 1303-1310.

(29) Kushida, Y.; Nagano, T.; Hanaoka, K. *Analyst* **2015**, *140*, 685-695.

(30) Yang, Y.; Lowry, M.; Xu, X.; Escobedo, J. O.; Sibrian-Vazquez, M.; Wong, L.; Schowalter, C. M.; Jensen, T. J.; Fronczek, F. R.; Warner, I. M.; Strongin, R. M. *Proc. Natl. Acad. Sci. U.S.A.* **2008**, *105*, 8829-8834.

(31) Stennett, E. M. S.; Ciuba, M. A.; Levitus, M. *Chem. Soc. Rev.* **2014**, *43*, 1057-1075.

(32) Zheng, Q.; Juette, M. F.; Jockusch, S.; Wasserman, M. R.; Zhou, Z.; Altman, R. B.; Blanchard, S. C. *Chem. Soc. Rev.* **2014**, *43*, 1044-1056.

(33) Escobedo, J. O.; Rusin, O.; Lim, S.; Strongin, R. M. *Curr. Opin. Chem. Biol.* **2010**, *14*, 64-70.

(34) Quek, C.-H.; Leong, K. W. *Nanomaterials* **2012**, *2*, 92-112.

(35) Guo, Z.; Park, S.; Yoon, J.; Shin, I. *Chem. Soc. Rev.* **2014**, *43*, 16-29.

(36) Liu, D.; Zhang, Z.; Zhang, H.; Wang, Y. *Chem. Commun.* **2013**, *49*, 10001-10003.

(37) Achelle, S.; Rodríguez-López, J.; F. Robin-Le Guen *J. Org. Chem.* **2014**, *79*, 7564-7571.

(38) Santos, F. M. F.; Rosa, J. N.; Candeias, N. R.; Carvalho, C. P.; Matos, A. I.; Ventura, A. E.; Florindo, H. F.; Silva, L. C.; Pischel, U.; Gois, P. M. P. *Chem. Eur. J.* **2016**, *22*, 1631-1637.

(39) Lim, C. W.; Tissot, O.; Mattison, A.; Hooper, M. W.; Brown, J. M.; Cowley, A. R.; Hulmes, D. I.; Blacker, A. J. *Org. Process Res. Dev.* **2003**, *7*, 379-384.

(40) Connolly, D. J.; Lacey, P. M.; McCarthy, M.; Saunders, C. P.; Carroll, A.-M.; Goddard, R.; Guiry, P. J. *J. Org. Chem.* **2004**, *69*, 6572-6589.

(41) Ramírez-López, P.; Ros, A.; Estepa, B.; Fernández, R.; Fiser, B.; Gómez-Bengoa, E.; Lassaletta, J. M. *ACS Catal.* **2016**, *6*, 3955-3964.

(42) Guram, A. S.; Buchwald, S. L. *J. Am. Chem. Soc.* **1994**, *116*, 7901-7902.

(43) Paul, F.; Patt, J.; Hartwig, J. F. *J. Am. Chem. Soc.* **1994**, *116*, 5969-5970.

(44) Ros, A.; Estepa, B.; Ramírez-López, P.; Álvarez, E.; Fernández, R.; Lassaletta, J. M. *J. Am. Chem. Soc.* **2013**, *135*, 15730-15733.

(45) Lippert, E. *Z. Naturforsch. A* **1955**, *10*, 541-545.

(46) Mataga, N.; Kaifu, Y.; Koizumi, M. *Bull. Chem. Soc. Jpn.* **1955**, *28*, 690-691.

(47) Mataga, N.; Kaifu, Y.; Koizumi, M. *Bull. Chem. Soc. Jpn.* **1956**, *29*, 465-470.

(48) Casida, M. E. In *Recent Advances in Density Functional Methods*; Chong, D. P., Ed.; World Scientific: Singapore, 1995; Vol. 1, p 155-192.

(49) Pais, V. F.; Lassaletta, J. M.; Fernández, R.; El-Sheshtawy, H. S.; Ros, A.; Pischel, U. *Chem. Eur. J.* **2014**, *20*, 7638-7645.

(50) Greenspan, P.; Fowler, S. D. *J. Lipid Res.* **1985**, *26*, 781-789.

(51) Sackett, D. L.; Wolff, J. *Anal. Biochem.* **1987**, *167*, 228-234.

(52) Belloc, F.; Dumain, P.; Boisseau, M. R.; Jalloustre, C.; Reiffers, J.; Bernard, P.; Lacombe, F. *Cytometry* **1994**, *17*, 59-64.

(53) Gaffield, M. A.; Betz, W. J. *Nat. Protocols* **2007**, *1*, 2916-2921.

(54) Nakamaru, K. *Bull. Chem. Soc. Jpn.* **1982**, *55*, 2697-2705.

## TOC Graph

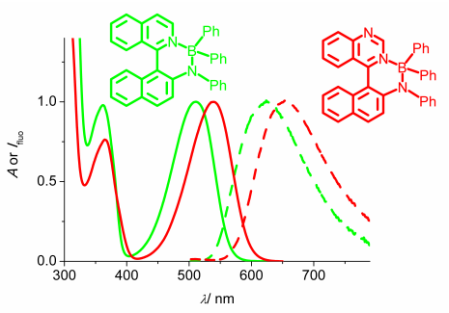
Ph
Ph
Ph
N
B
N
Ph
Ph
Ph
N
N
B
N
Ph
1.0
0.5
0.0
A or I_fluo
300
400
500
600
700
λ/ nm